sustainability

MDPI

Article

Air Quality Index (AQI) Prediction in Holy Makkah Based on Machine Learning Methods

Abdulrazak H. Almaliki [1], Abdessamed Derdour [2,3] and Enas Ali [4,*]

[1] Department of Civil Engineering, College of Engineering, Taif University, P.O. Box 11099, Taif 21944, Saudi Arabia; a.almaliki@tu.edu.sa
[2] Artificial Intelligence Laboratory for Mechanical and Civil Structures and Soil, University Center of Naama, P.O. Box 66, Naama 45000, Algeria; derdour@cuniv-naama.dz
[3] Laboratory for the Sustainable Management of Natural Resources in Arid and Semi-Arid Zones, University Center Salhi Ahmed Naama (Ctr Univ Naama), P.O. Box 66, Naama 45000, Algeria
[4] Faculty of Engineering and Technology, Future University in Egypt, New Cairo 11835, Egypt
* Correspondence: enas.ali@fue.edu.eg

Abstract: Makkah draws millions of visitors during Hajj and Ramadan, establishing itself as one of Saudi Arabia's most bustling cities. The imperative lies in maintaining pristine air quality and comprehending diverse air pollutants to effectively manage and model air pollution. Given the capricious and variably spatiotemporal nature of pollution, predicting air quality emerges as a notably intricate endeavor. In this study, we confronted this challenge head-on by harnessing sophisticated machine learning techniques, encompassing the fine decision tree (FDT), ensemble boosted tree (EBOT), and ensemble bagged tree (EBAT). These advanced methodologies were enlisted to project air quality index (AQI) levels, focusing specifically on the Makkah region. Constructed and trained on air quality data spanning 2016 to 2018, our forecast models unearthed noteworthy insights. The outcomes revealed that EBOT exhibited unparalleled accuracy at 97.4%, astutely predicting 75 out of 77 samples. On the other hand, FDT and EBAT achieved accuracies of 96.1% and 94.8%, respectively. Consequently, the EBOT model emerges as the epitome of reliability, showcasing its prowess in forecasting the air quality index. We believe that the insights garnered from this research possess universal applicability, extending their potential to regions worldwide.

Keywords: Makkah; EBOT; FDT; EBAT; prediction

Citation: Almaliki, A.H.; Derdour, A.; Ali, E. Air Quality Index (AQI) Prediction in Holy Makkah Based on Machine Learning Methods. *Sustainability* **2023**, *15*, 13168. https://doi.org/10.3390/su151713168

Academic Editor: Giouli Mihalakakou

Received: 20 July 2023
Revised: 24 August 2023
Accepted: 31 August 2023
Published: 1 September 2023

1. Introduction

Respiratory diseases are among the many health risks of polluted air [1,2]. Each year, around 7 million people worldwide die from air pollution [3]. In addition, air pollution can cause global warming, which is the process by which heat is trapped in the air, resulting in temperature increases, rising sea levels, and diseases caused by the hot climate [4]. As a worldwide emergency, climate change can only be solved by collaboration between countries [5]. As the United Nations Framework Convention on Climate Change (UNFCCC) mentioned, 195 countries signed the Paris Climate Agreement or COP21 in December 2015, and 190 approved it as of January 2021 [6]. By supporting this agreement, the world moves toward net-zero emissions and achieving sustainable development goals [7]. All countries have pledged to reduce emissions and work together to adapt to climate change [7]. Consequently, countries submitted nationally determined contributions for climate action in 2020. For example, Saudi Arabia, which ranks tenth in carbon dioxide (CO_2) emissions and is the world's largest exporter of fossil fuels, promised to reduce its carbon emissions to zero, so greenhouse gases will not be added to the atmosphere, by 2060 [8].

The air quality index (AQI) is a pivotal metric for evaluating air quality. It plays a crucial role in assessing the cleanliness of the air by quantifying various pollutants and their

potential health impacts. Through the calculation of AQI, a comprehensive understanding of air quality levels is attained, enabling informed decisions and actions to safeguard public health and the environment [9]. By warning people whenever the AQI exceeds the maximum value, we can prevent people from being affected by pollution. As a result of the AQI, people are warned about the quality of the air in which they live and given information about what groups may be affected by the air and some steps they can take to prevent it. Polluted air can have various health effects within hours to days of breathing it [10]. AQI is used to determine how quickly people could be affected by it. In order to calculate the air quality index, six pollutants are generally taken into account: ozone (O_3), sulfur dioxide (SO_2), carbon monoxide (CO), fine particulate matter ($PM_{2.5}$), nitrogen dioxides (NO_2), and inhalable particles (PM_{10}) [11]. AQI values range from 0 to 500 based on a random scale [12]. Air pollution levels and health concerns are generally higher when the AQI is high. When the air quality index is 50 or less, it is considered good, while when the index is 300 or greater, it is considered hazardous [12]. Health concerns are classified according to AQI according to six categories. The categories are color-coded so that they can be easily understood. It takes time and effort to manage and solve air pollution problems. It is possible to prevent damage caused by air pollution through air quality forecasts. In order to prevent serious pollution incidents, it is important for air quality forecasting to be completed on time. There are many machine learning algorithms available for predicting data. An algorithm is trained to understand patterns in data and make decisions based on this information in machine learning. The three main types of machine learning are supervised, unsupervised, and semi-supervised. Big data predictions made with machine learning have become increasingly popular [13]. Several researchers have successfully forecasted air quality using machine learning algorithms [14–16]. Multilayer neural networks were used by Pérez et al. [17] to predict $PM_{2.5}$ concentrations hourly in Chile. Ragab et al. [15] used a novel one-dimensional CNN with exponential adaptive gradients to predict air pollution index. The air quality index (AQI) in Milan, Italy, was predicted using feed-forward neural networks by Corani [18]. A publicly health-oriented air quality forecasting model based on MLP type neural networks was developed by Hrust et al. [19] in Zagreb, Croatia. Artificial neural networks and multiple regression models were used to forecast the hourly PM_{10} concentration in Cyprus by Paschalidou et al. [20]. Liu et al. [21] predicted the air quality index (AQI) in Beijing by using random forest regression (RFR) and support vector regression (SVR).

The primary aim of this study is twofold: Firstly, to evaluate the air quality index (AQI) in Makkah, Saudi Arabia, considering key pollutants such as PM_{10}, NO_2, CO, SO_2, and O_3. Secondly, the study introduces a novel methodology for forecasting AQI utilizing machine learning algorithms. The forecasted AQI results are categorized into distinct levels from "good" to "hazardous," and the accuracy of both computed and forecasted AQI values is rigorously assessed. This research seeks to contribute to effective air quality management by enhancing our understanding of AQI dynamics and providing reliable forecasting mechanisms for informed decision-making and public health safeguarding.

2. Materials and Methods

2.1. Study Area and Data Used

Worldwide, Makkah is regarded as a holy city by Muslims. With a total area of about 1.200 km^2 and an elevation of 277 m above sea level, Makkah City is the administrative capital of the Makkah Region, located 80 km from the Red Sea. Its geographical location lies between 39°41.867′ E and 39°53.961′ E and 21°20.646′ N and 21°31.107′ N. Makkah City has quite complex topography because of the many mountains surrounding the residential area around Haram Mosque. In 2017, Makkah City had a population of 2,017,793, covering 333.54 km^2 according to the census, where approximately 70% of population lives in urban areas. It is almost twice as large as it was in 2003 [22]. Approximately three million people from around the world visit Makkah annually for the pilgrimage "Hajj" [23]. A total of 19.2 million pilgrims participated in the Umrah rite during the other months of the

year; nonetheless, pilgrims are more prevalent during the holy month of Ramadan (9th month of the Islamic calendar) [24]. Traffic congestion caused by pilgrims causes high levels of exhaust and non-exhaust emissions, leading to high levels of dust resuspension throughout the city [25]. The summer season in Makkah is hot and dry, with maximum temperatures reaching 55 degrees Celsius, like the rest of Saudi Arabia [26]. The average annual precipitation in Makkah is 89.4 mm between September and January [26]. In this study, as shown in Figure 1, mean hourly air quality data was collected at Haram station, located near the Holy Mosque (Al-Haram), from January 2016 to December 2018. It is located in the eastern yard of the Grand Holy Mosque, at 21°25′28.7″ N 39°49′45.0″ E. The location is an active monitoring station that analyzes the quantities of NOx, NO, NO_2, SO_2, CO, O_3, and PM_{10}.

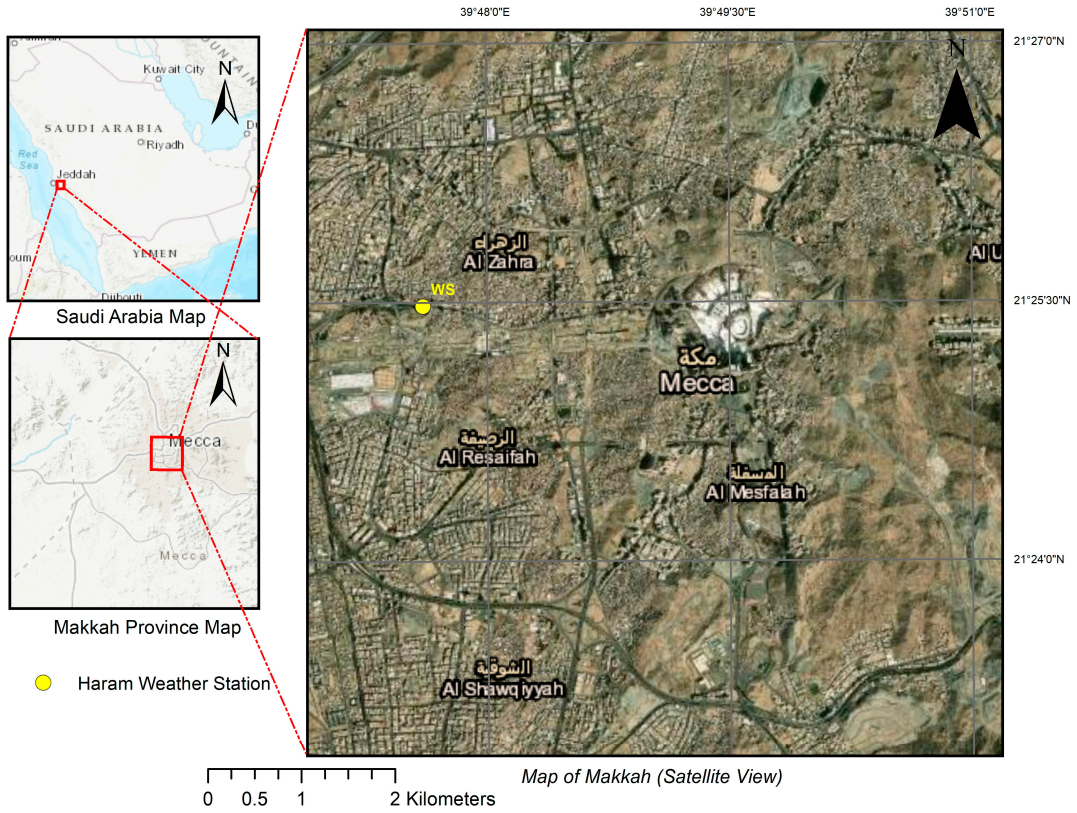

Figure 1. Study area.

2.2. Air Quality Index Calculation

The air quality index (AQI) is a comprehensive measure of air pollution, encompassing pollutants such as NO_2, CO, SO_2, O_3, and PM_{10}, known for their acute health impacts [27]. Designed to offer daily guidance on avoiding short-term health issues, AQI is calculated by converting pollutant concentrations using a piecewise linear function [28]. The AQI sub-index, denoted as $I_{P,S}$, is computed for each pollutant and station using Equation (1), considering concentration breakpoints (C_{High} and C_{Low}), pollutant concentration (C_P), and corresponding breakpoint indices (I_{High} and I_{Low})

$$I_{P,S} = \frac{I_{High} - I_{Low}}{C_{High} - C_{Low}}(C_P - C_{Low}) + I_{Low} \quad (1)$$

AQI is then determined for each station as the maximum value among sub-indices, as shown in Equation (2).

$$AQI_S = \max\left(I_{O_3},\ I_{PM10}\ ,\ I_{CO}\ ,\ I_{so_2}, I_{NO_2}\right) \quad (2)$$

AQIs range from 0 to 500 on a standardized scale. Higher AQI values correspond to elevated pollution levels and increased health concerns. For instance, AQI values ≤ 50 indicate "good" air quality, while values ≥ 300 are considered "hazardous". Six color-coded categories simplify AQI interpretation for the public as shown in Table 1.

Table 1. Ranges of the AQI class.

Code	State	AQI Range
1	Good	AQI < 50
2	Moderate	50 < AQI < 100
3	Unhealthy for sensitive groups	100 < AQI < 150
4	Unhealthy	150 < AQI < 200
5	Very Unhealthy	200 < AQI < 300
6	Hazardous	AQI > 300

Figure 2 is the flow chart that shows the operation of the constructed model to develop the predictive classification model. The model operation is based on computing the AQI using Equations (1) and (2). Therefore, the parameters for each sample, NO_2, CO, SO_2, O_3, and PM_{10}, were used with the AQI as the classifiers as training data. The classifier, which develops the highest classification accuracy, will predict the new data and investigate its robustness.

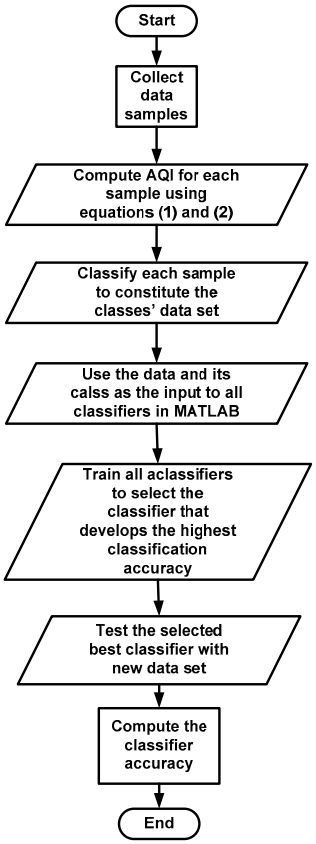

Figure 2. Model operation flowchart.

2.3. Classification Learners

Classification algorithms are used in data analysis and machine learning to predict or categorize new instances based on the patterns and relationships seen in a labeled training dataset. Classification methods are beneficial when the target variable or desired outcome is discrete or categorical. Classification methods offer a systematic and structured approach to categorizing new instances based on historical patterns, enabling decision-making, pattern

recognition, and prediction in various domains such as healthcare, finance, marketing, engineering applications, and more. The current study's methodology was focused on forecasting the AQI in Makkah to look into the pollution during the busiest periods of seasonal celebrations like the Haj and Umrah in Ramadan. The classification techniques frequently used as classifiers are used to predict the AQI.

Models for the classifiers, decision trees, ensembles, support vector machines, closest neighbors, and neural networks may all be trained using MATLAB's classification learner toolbox. It can also study the data, define characteristics, specify validation protocols, and assess results. It presents the results of various classifications, one or all of which have been chosen. Diagnostic tools use a scatter plot or confusion matrix to visualize the results of the selected or all models. By aggregating all available classification models, we derive a comprehensive accuracy assessment across the entire model spectrum. This process enables us to discern the most adept model, which is subsequently harnessed to assess fresh data, exporting its predictive prowess to anticipate outcomes. In the ongoing investigation, the dataset encapsulates air composition data, meticulously gathered from the revered pollution monitoring station in holy Makkah. The data were collected over three years, from 2016 to 2018. The data contained the concentration of some gases in the atmosphere, which are used to identify the air quality index. These gases are NO_2, CO, SO_2, O_3, and PM_{10}. The collected data included 1096 samples recorded daily from 1 January 2016 to 31 December 2018. This data is divided into two parts: the training part included 1019 data samples, and the testing part included 77 data samples. These data were utilized to determine the air quality index (AQI) and then classified into six categories based on the range of AQI in Table 1. The six classes are good, moderate, unhealthy for sensitive groups, unhealthy, very unhealthy, and hazardous AQI state, coded to 1, 2, 3, 4, 5, and 6, respectively. Table 2 shows the number of samples in each class for training and testing for classification purposes (1019 samples for training and 77 samples for testing). A total of 1096 data samples were collected daily from 1 January 2016 to 31 December 2018. Then, the AQI for each sample was computed and then the AQI for each sample were classified into six groups, as mentioned above. If 1096 was divided by 3 years, it gives 365 days, which refers to the days of the year. Several selected training data are illustrated in Table 3.

Table 2. Number of samples in each class for training and testing purposes.

	Training	Testing	Total
1	113 (11.089%)	20 (25.97%)	133 (12.135%)
2	438 (42.983%)	20 (25.97%)	458 (41.788%)
3	295 (28.949%)	20 (25.97%)	315 (28.740%)
4	87 (8.538%)	10 (12.99%)	97 (8.85%)
5	72 (7.066%)	5 (6.49%)	77 (7.026%)
6	14 (1.373%)	2 (2.61%)	16 (1.461%)
Total	1019	77	1096

Table 3. Several training samples.

Date	NO_2	CO	SO_2	O_3	PM 10	AQI Value	AQI Category
1-Jan	7.55	0.06	3.56	26.86	88.10	90.02	Moderate
2-Jan	19.01	0.29	3.48	18.78	176.27	176.27	Unhealthy
3-Jan	11.10	0.01	3.94	19.63	82.10	82.10	Moderate
4-Jan	16.69	0.38	3.12	15.28	153.74	153.74	Unhealthy
5-Jan	22.35	0.24	6.27	18.98	105.22	105.22	Unhealthy for sensitive groups
6-Jan	13.71	0.15	2.37	17.85	87.42	87.42	Moderate
7-Jan	9.13	0.29	3.62	18.70	125.45	125.45	Unhealthy for sensitive groups
8-Jan	11.59	0.23	1.62	16.16	121.62	121.89	Unhealthy for sensitive groups
9-Jan	16.55	0.84	1.05	15.78	6.34	28.93	Good
7-Oct	201.0	15.5	0.1	3.8	17.9	201.0	Very Unhealthy
2-Dec	93.9	36.7	1.0	148.9	17.7	219.5	Very Unhealthy
6-Aug	20.45	0.55	1.48	16.91	342.50	342.50	Hazardous
16-Sep	11.58	0.78	1.00	19.07	412.08	412.70	Hazardous

All classifiers in the classification learner's toolbox were applied to the training data. When the accuracy results of each class were obtained, the best classifiers were selected and then used for the testing data. The training data were classified into 113, 438, 295, 87, 72, and 14 samples for good, moderate, unhealthy for sensitive groups, unhealthy, very unhealthy, and hazardous AQI states. The accuracy results of applying all classifiers to the training data indicated that three classifiers developed a higher prediction accuracy than the others and gave the same prediction accuracy of 95.6%. These classifiers were the fine decision tree (FDT), ensemble boosted tree (EBOT), and ensemble bagged tree (EBAT). Figures 3 and 4 show the scatter plot of the classifier to indicate the accuracy results of all classifiers. It indicated that the fine decision tree developed the highest accuracy, followed by the ensemble boosted tree and the ensemble bagged tree. The circles and crosses referred to the correct and incorrect predictions of the samples. Therefore, we will review the results of the three classifiers through the confusion matrix and the ROC curves.

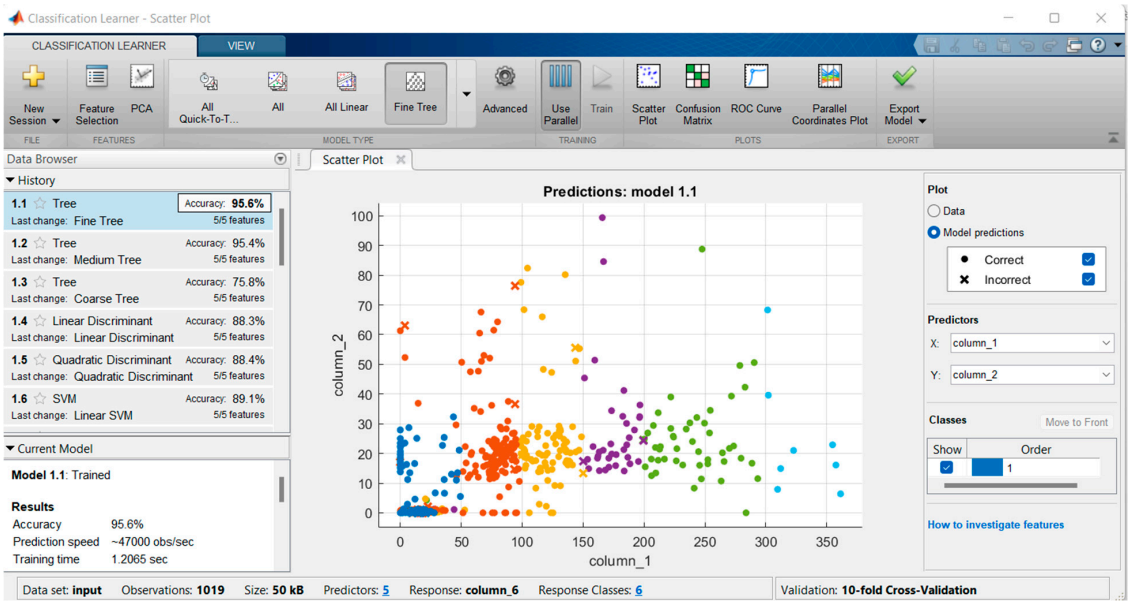

Figure 3. Scatter plot for fine decision tree.

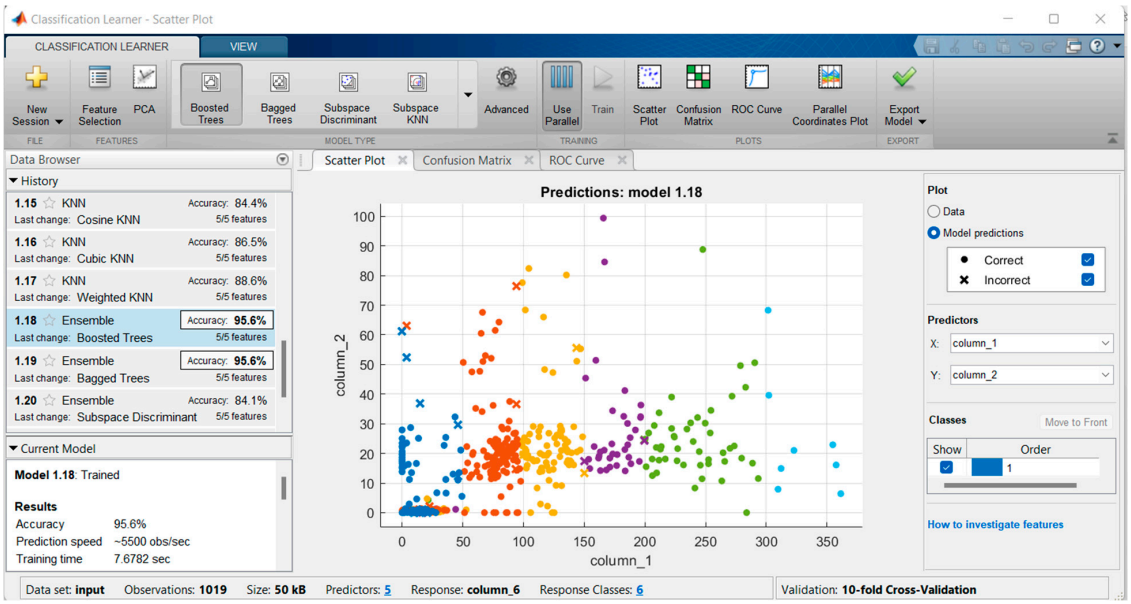

Figure 4. Scatter plot for ensemble boosted and bagged trees.

2.4. Decision Tree

A decision-learning tree is a predictive modeling method used in statistics, data mining, and machine learning. Variables take on a separate set of values in decision trees called classification trees. In a tree, the leaves represent specific categories, and the branches represent logical associations for the characteristics that lead to those categories. Decision trees targeting numerical variables with continuous values (real numbers) are called regression trees (relative to linear regression). A decision tree can be used in decision analysis to represent decisions and decision-making processes visually. In data mining, decision trees describe the data (but the output of the classification tree can be an input to the decision-making process). Regression is widely used in science and engineering because of its ease of visualization. The decision tree algorithm falls into the category of supervised learning algorithms. However, unlike supervised learning algorithms, decision tree algorithms can also solve regression and classification problems. The general motivation for using a decision tree is to create a training model to predict the class or value of target variables using learning decision rules inferred from previous data (training data). The level of understanding of the decision tree algorithm is elementary compared to other classification algorithms. The decision tree algorithm tries to solve the problem using tree representation. Each inner node of the tree corresponds to a feature, and each leaf node corresponds to a class label.

In decision trees as shown in Figure 5, the tree's root is the starting point to predict the variable of any class label for a record. Then, the values of the root's attribute are compared with the record's attribute. Based on the comparison, we follow the branch corresponding to that value was followed and move to the next node. Then, compare the record attributes' values with other internal tree nodes until a leaf node with an expected class value is reached. We also know how a model decision tree can predict the target class or value. Now let us understand how we can create a decision tree model.

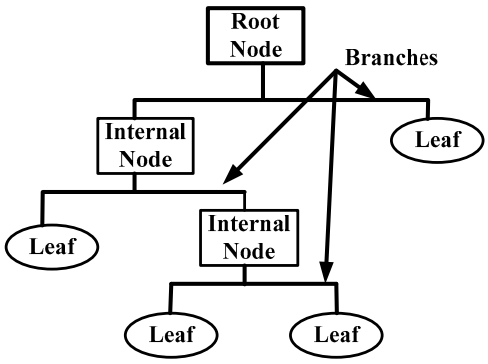

Figure 5. Decision tree model.

Assumptions while creating a decision tree:

- Here are some of the assumptions we make while using a decision tree:
- Initially, the entire training set is considered a root.
- Feature values are best divided into categories. If the values are continuous, they will be estimated before the model is generated.
- Records are distributed recursively based on attribute values.
- The positioning of the attributes is arranged as the root or internal node of the tree using some tools of statistical approach.

2.5. Ensemble Trees

Instead of using a single decision tree to predict the decision, some trees are grouped to achieve good predictive performance where some weak learners can combine to form strong learners and then enhance their decision-making. There are two techniques to perform an ensemble decision tree: one is bagging, and the other is boosting.

2.6. Ensemble Bagged Tree

The bagging method can be used when our goal is to reduce the decision tree's variance. It relies on creating several subsets of data from the training sample randomly selected with replacement. Hence, each sub-data set is used to train its own decision tree, and then a set of results for different models are developed. Then, the average of those predictions from different trees is used to produce the decision, which is better than the decision based on a single decision tree. Figure 6 explains that the ensemble packing tree classifier can be generated by preparing the data samples as training data in random form. Then, the decision tree is trained to obtain the base model with or without cross-validation, and the voting method combines each base model. The main concept of voting is to generalize better by compensating for individual model errors separately.

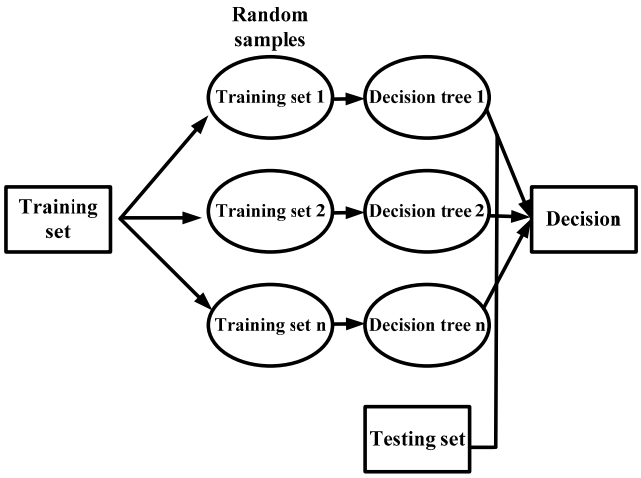

Figure 6. Flowchart of ensemble bagging tree.

2.7. Ensemble Boosted Tree

The boosting method is one of the methods used in ensemble trees to construct a prediction tree. In this method, the learners learn sequentially with the first learners who have installed simple data models and then search for the error by analyzing that data. In this method, we fit successive trees (random samples), and at each step, we try to reach the lowest value of errors from the prior tree, which is the main goal. Figure 7 depicts the boosting tree and explains how to generate one improved model every time with fewer errors. However, the boosting models with fewer errors can be overfitted because they modifies themselves.

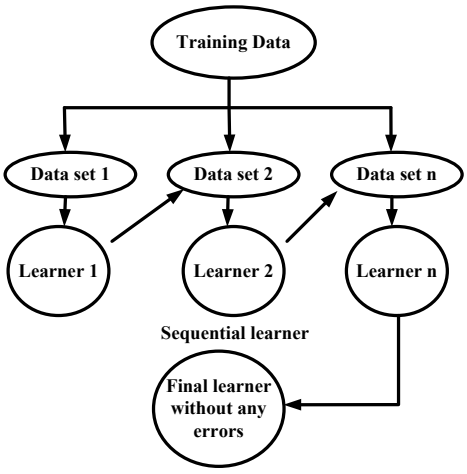

Figure 7. Ensemble boosting tree flowchart.

3. Results and Discussion

3.1. Air Quality Index Results

The present research investigates air pollution data extracted from the Haram station, which is located nearby the Holy Mosque (Al-Haram) in Makkah in Saudi Arabia, which is used to calculate the air quality index (air pollution index) in terms of critical parameters. This dataset possesses observations from January 2016 to December 2018. Table 4, presented below, provides brief descriptive statistics of the pollutants ($PM_{2.5}$, PM_{10}, NO_2, CO, SO_2, O_3) and the results of AQI from this dataset. We remark that the AQI values ranged from 5.02 to 430, with a mean of 101.22 in 2016. AQI varied from to 1.50 to 346.12 with an average of 103.95 in 2017, while the values of AQI were ranged from 0.00 to 361.38 with a mean of 120.67 in 2018. High values of AQI were registered during the period of Hajj. This may be attributed to heavy traffic and extensive human activities in this period, as more than three million people visit Makkah in this period.

Table 4. Descriptive statistics of the pollutants and AQI.

		NO_2	CO	SO_2	O_3	PM_{10}	AQI Value
2016	Min	1.08	0.00	0.00	0.00	0.00	5.02
	Max	31.46	4.71	16.65	38.99	430.00	430.00
	Mean	15.39	0.27	2.77	18.12	97.86	101.22
	S.d	4.59	0.45	2.04	5.71	60.17	57.30
2017	Min	0.00	0.00	0.00	0.00	0.00	1.50
	Max	52.81	1.59	28.91	105.57	346.12	346.12
	Mean	17.58	0.49	4.13	18.60	102.70	103.95
	S.d	6.82	0.34	2.74	9.45	47.58	46.86
2018	Min	0.00	0.00	0.00	0.00	0.00	0.00
	Max	361.38	99.40	3.17	148.90	52.13	361.38
	Mean	115.13	23.29	0.43	4.74	19.33	120.67
	S.d	79.54	16.69	0.42	8.41	8.15	74.77

3.2. Machine Learning Algorithms Results

Fine Decision Tree

The confusion matrix of the fine decision tree presented the FDT performance. Each column of the matrix presents the number of predictions of each AQI class (1: good, 2: moderate, 3: unhealthy for sensitive groups, 4: unhealthy, 5: very unhealthy, and 6: hazardous), while each row represents the instances in the real class. The confusion matrix indicates the successes of the predictive model. Figure 8 shows the confusion matrix of FDT that illustrates the number of correct and incorrect predictors of the trained samples. As shown in Figure 8, the correct predictions appeared in green and the incorrect predictions appeared in red. For example, for class 4, referring to the unhealthy AQI state, the FDT can correctly predict 79 of 87 samples, while 8 samples were incorrect predictions (six indicated unhealthy for sensitive groups AQI state and two samples for very unhealthy AQI state). The prediction accuracy can be illustrated in the confusion matrix in Figure 9.

The percentage of the true positive rate (TPR) in green and the false negative rate (FNR) in red is shown in Figure 9. The FNR refers to the error rate, explaining the probability that a TPR will miss. On the other hand, TPR measures the metric sensitivity referring to the likelihood that actual positive results are achieved. For example, it is shown in Figure 9 that class 4 (unhealthy AQI state) has a true positive rate (TPR) of sensitivity of 91% and a false negative rate (FNR) of 9%. Therefore, the constructed FDT model can discriminate between TPR and FNR with an accuracy of 91%. On the other hand, the highest TPR sensitivity can be observed in the case of class 5 (very unhealthy AQI state) where the TPR is 96% with an FNR of 4%.

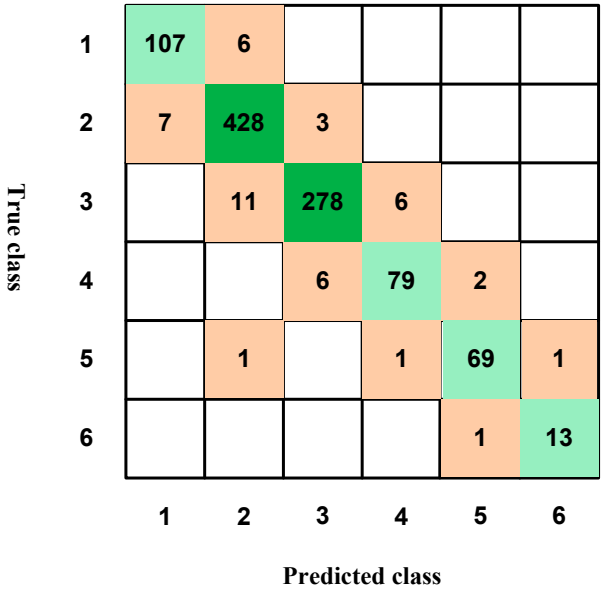

Figure 8. Confusion matrix of FDT (green color for correct prediction and red color for incorrect prediction).

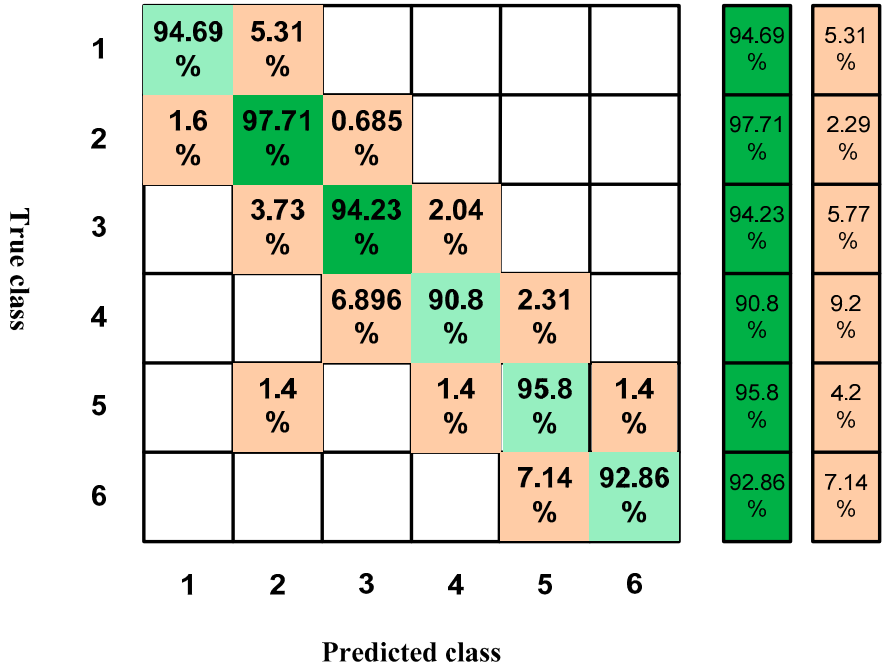

Figure 9. Confusion matrix based on TPR and FNR rates (green color for correct prediction and red color for incorrect prediction).

The positive predictive value (PPV) and the false discovery rate (FDR) can be illustrated in Figure 10. These measures the accuracy of the prediction model for classification purposes. It should be considered that higher accuracy can be obtained with a lower dispersion value. For example, the predictive FDT model for class 3 (unhealthy for sensitive groups) shows the highest precision value of 97% and an FDR percentage of 3%. It correctly classified class 3 as class 397% of the time, and it predicted incorrectly with classes 2 and 4 with 1 and 2% false prediction, respectively. The receiver operating curve (ROC) of class 1 of FDT is illustrated in Figure 11. It is used to indicate the accuracy of the constructed FDT model. It explains the cut-off point of a continuous scale. When the ROC makes a right angle, it refers to high accuracy; if this angle is 45°, it indicates bad model accuracy. The

area under the curve (AUC) is a key measure of the accuracy of the FDT model: when the AUC is 1, it means better model performance. The marker on ROC depicts the current classifier performance, where the false positive rate (FPR) is on the x-axis, and the true positive rate (TPR) is on the y-axis. For example, Figure 11 depicts that the FPR is 0.01, referring to 1% of the observations being assigned incorrectly to the positive class. The TPR of 0.95 indicates that the classifier correctly assigns 95% of the observations to the positive class. In that sense, in Figure 10, the ROC graph for class 1 (dissatisfied) is shown.

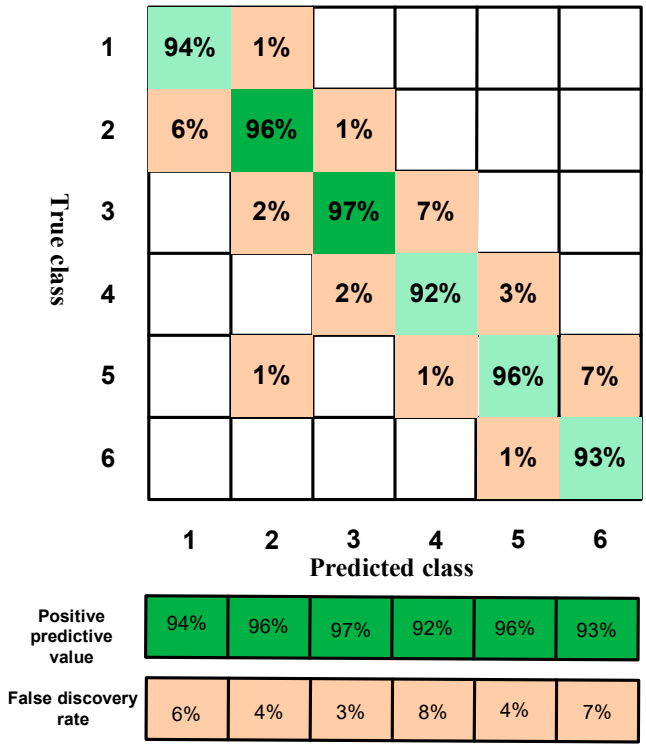

Figure 10. Confusion matrix based on PPV and FDR rates (green color for correct prediction and red color for incorrect prediction).

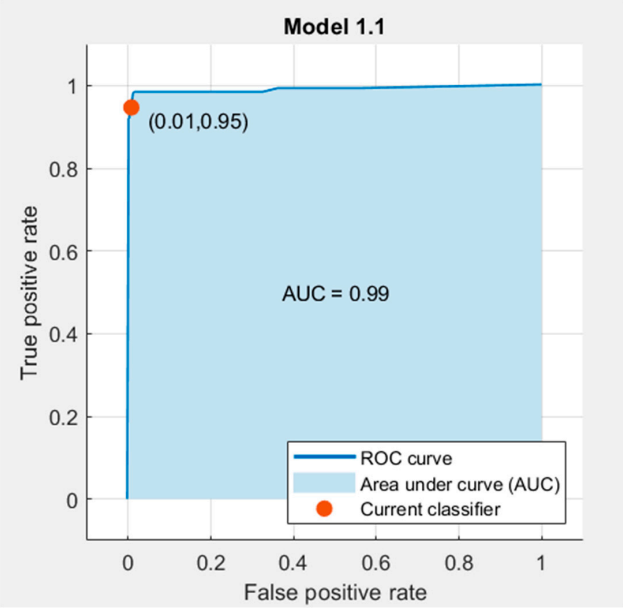

Figure 11. The AUC curve for class 1 of the DFT model.

The same confusion matrices were also developed for EBOT and EBAT as for that of FDT, but we did not explain it again. So, we compare the results of the three classifiers in table form. Table 5 compares the classifiers for predicting the highest accuracy results based on the applied data samples. Table 5 shows that the three classifiers develop the same prediction accuracies of 95.6%.

Table 5. The classifiers' accuracies based on training data.

AQI State	FDT	EBOT	EBAT
Good	107/113 (95%)	112/113 (99%)	108/113 (96%)
Moderate	428/438 (98%)	423/438 (79%)	425/438 (97%)
Unhealthy for sensitive groups	278/295 (94%)	279/295 (95%)	282/295 (96%)
Unhealthy	79/87 (91%)	78/87 (90%)	79/87 (91%)
Very Unhealthy	69/72 (96%)	69/72 (96%)	69/72 (96%)
Hazardous	13/14 (93%)	13/14 (93%)	11/14 (79%)
Overall	974/1019 (95.6%)	974/1019 (95.6%)	974/1019 (95.6%)

Although the three models' overall prediction accuracy were the same, the accuracy of predicting each AQI state was different. For example, the AQI good state accuracy of FDT was 95 for FDT. This was 99 and 96% for EBOT and EBAT, respectively. The AQI state accuracy was identified by dividing the correct prediction states by the overall samples of the state, e.g., the accuracy of AQI moderate state for EBOT is 423 correct samples out of 438 total samples. The accuracy of the three classifiers can be verified using test data samples. Table 6 displays the testing data, whereas Table 7 presents the prediction accuracy results for the same testing data. The results indicated that the EBOT developed the highest accuracy of 97.4%, which correctly predicted 75 of 77 samples. The FDT and EBAT developed accuracies of 96.1 and 94.8%, respectively. Therefore, EBOT is considered the best classifier model for applying data.

Table 6. Testing data samples.

Date	NO_2	CO	SO_2	O_3	PM 10	AQI Value	AQI Category
19-Oct	10.31	0.00	2.60	25.49	40.00	41.70	Good
24-Oct	12.84	0.00	1.76	16.54	36.40	43.77	Good
25-Oct	16.11	0.00	2.33	22.49	40.17	49.05	Good
8-Mar	13.61	0.26	1.19	17.08	60.85	61.38	Moderate
9-Mar	16.55	0.66	1.23	11.85	63.69	74.73	Moderate
16-Mar	11.23	0.15	3.66	19.12	118.05	118.05	Unhealthy for sensitive groups
20-Mar	17.91	0.19	5.11	13.69	113.96	113.96	Unhealthy for sensitive groups
29-May	16.68	0.74	3.05	14.42	184.15	184.15	Unhealthy
31-May	14.30	0.33	3.72	14.07	193.56	193.56	Unhealthy
12-Mar	7.77	0.65	3.11	14.62	214.68	214.68	Very Unhealthy
22-Mar	18.12	0.46	2.30	18.40	276.38	276.38	Very Unhealthy
2-Jan	325.2	45.5	0.1	3.1	12.2	325.2	Hazardous
30-Jan	333.9	78.3	0.1	6.7	24.5	333.9	Hazardous

Table 7. The classifiers' accuracies based on testing data.

AQI State	FDT	EBOT	EBAT
Good	18/20 (90%)	20/20 (99%)	18/20 (90%)
Moderate	20/20 (100%)	20/20 (79%)	19/20 (95%)
Unhealthy for sensitive groups	19/20 (95%)	18/20 (90%)	19/20 (95%)
Unhealthy	10/10 (100%)	10/10 (100%)	10/10 (100%)
Very Unhealthy	5/5 (100%)	5/5 (100%)	5/5 (100%)
Hazardous	2/2 (100%)	2/2 (100%)	2/2 (100%)
Overall	74/77 (96.1%)	75/77 (97.4%)	73/77 (94.8%)

4. Conclusions

This study delved into three years (2016–2018) to comprehensively assess air pollution levels in Makkah. The utilization of the air quality index (AQI) served as a vital tool, offering both the public and decision makers an understandable gauge of air quality. Given pollution's intricate and ever-changing nature across time and space, accurately predicting air quality is formidable. Yet, our study successfully tackled this challenge through the strategic application of advanced machine learning techniques, specifically employing the fine decision tree (FDT), ensemble boosted tree (EBOT), and ensemble bagged tree (EBAT) models. These sophisticated methodologies were harnessed to craft predictive models for the AQI in the Makkah region. Drawing insights from air quality data from 2016 to 2018, our models unveiled significant revelations. Notably, the EBOT model demonstrated unparalleled accuracy, boasting an impressive 97.4% success rate by adeptly forecasting 75 out of 77 samples. Complementarily, the FDT and EBAT models secured accuracies of 96.1% and 94.8%, respectively.

The unequivocal success of the EBOT model positions it as the cornerstone of reliability in forecasting the air quality index. This achievement not only underscores the efficacy of machine learning in predicting air quality but also underscores the potential for mitigating environmental issues through innovative approaches. As a logical next step, we propose a more in-depth exploration of hourly data to enhance predictive outcomes and elevate performance standards. The insights garnered from our research carry universal applicability, presenting opportunities to address air quality concerns on a global scale. By embracing the synergy between machine learning and environmental management, we pave the way for a sustainable and healthier future.

Author Contributions: Conceptualization, A.H.A., A.D. and E.A.; Data curation, A.H.A., A.D. and E.A.; Formal analysis, A.H.A., A.D. and E.A.; Funding acquisition, A.H.A.; Investigation, A.H.A., A.D. and E.A.; Methodology, A.H.A., A.D. and E.A.; Project administration, A.H.A., A.D. and E.A.; Resources, A.H.A., A.D. and E.A.; Software, A.H.A., A.D. and E.A.; Supervision, A.H.A., A.D. and E.A.; Validation, A.H.A., A.D. and E.A.; Visualization, A.H.A., A.D. and E.A.; Writing—original draft, A.H.A., A.D. and E.A.; Writing—review and editing, A.H.A., A.D. and E.A. All authors have read and agreed to the published version of the manuscript.

Funding: This work is funded by the Deanship of Scientific Research, Taif University.

Institutional Review Board Statement: Not applicable.

Informed Consent Statement: Not applicable.

Data Availability Statement: Not applicable.

Acknowledgments: The researchers would like to acknowledge the Deanship of Scientific Research, Taif University for funding this work.

Conflicts of Interest: The authors declare no conflict of interest.

References

1. Kim, D.; Chen, Z.; Zhou, L.-F.; Huang, S.-X. Air pollutants and early origins of respiratory diseases. *Chronic Dis. Transl. Med.* **2018**, *4*, 75–94. [CrossRef]
2. Simkovich, S.M.; Goodman, D.; Roa, C.; Crocker, M.E.; Gianella, G.E.; Kirenga, B.J.; Wise, R.A.; Checkley, W. The health and social implications of household air pollution and respiratory diseases. *npj Prim. Care Respir. Med.* **2019**, *29*, 12. [CrossRef]
3. Lelieveld, J.; Haines, A.; Pozzer, A. Age-dependent health risk from ambient air pollution: A modelling and data analysis of childhood mortality in middle-income and low-income countries. *Lancet Planet. Health* **2018**, *2*, e292–e300. [CrossRef]
4. Jacobson, M.Z. *Air Pollution and Global Warming: History, Science, and Solutions*; Cambridge University Press: Cambridge, UK, 2012.
5. Hoffmann, M.J. *Climate Governance at the Crossroads: Experimenting with a Global Response after Kyoto*; Oxford University Press: Oxford, UK, 2011.
6. Conference of the Parties (COP). United Nations Climate Change Conference. 2021.
7. Sofuoğlu, E.; Kirikkaleli, D. Towards achieving net zero emission targets and sustainable development goals, can long-term material footprint strategies be a useful tool? *Environ. Sci. Pollut. Res.* **2022**, *30*, 26636–26649. [CrossRef] [PubMed]

8. Rahman, M.M.; Hasan, M.A.; Shafiullah, M.; Rahman, M.S.; Arifuzzaman, M.; Islam, M.K.; Islam, M.M.; Rahman, S.M. A Critical, Temporal Analysis of Saudi Arabia's Initiatives for Greenhouse Gas Emissions Reduction in the Energy Sector. *Sustainability* **2022**, *14*, 12651. [CrossRef]
9. Plaia, A.; Ruggieri, M. Air quality indices: A review. *Rev. Environ. Sci. Bio/Technol.* **2011**, *10*, 165–179. [CrossRef]
10. Thurston, G.D.; Kipen, H.; Annesi-Maesano, I.; Balmes, J.; Brook, R.D.; Cromar, K.; De Matteis, S.; Forastiere, F.; Forsberg, B.; Frampton, M.W. A joint ERS/ATS policy statement: What constitutes an adverse health effect of air pollution? An analytical framework. *Eur. Respir. J.* **2016**, *49*, 1600419. [CrossRef]
11. Sheng, N.; Tang, U.W. The first official city ranking by air quality in China—A review and analysis. *Cities* **2016**, *51*, 139–149. [CrossRef]
12. Kumar, A.; Goyal, P. Forecasting of daily air quality index in Delhi. *Sci. Total Environ.* **2011**, *409*, 5517–5523. [CrossRef]
13. Wu, Q.; Lin, H. A novel optimal-hybrid model for daily air quality index prediction considering air pollutant factors. *Sci. Total Environ.* **2019**, *683*, 808–821. [CrossRef]
14. Iskandaryan, D.; Ramos, F.; Trilles, S. Air quality prediction in smart cities using machine learning technologies based on sensor data: A review. *Appl. Sci.* **2020**, *10*, 2401. [CrossRef]
15. Ragab, M.G.; Abdulkadir, S.J.; Aziz, N.; Al-Tashi, Q.; Alyousifi, Y.; Alhussian, H.; Alqushaibi, A. A novel one-dimensional cnn with exponential adaptive gradients for air pollution index prediction. *Sustainability* **2020**, *12*, 10090. [CrossRef]
16. Yu, R.; Yang, Y.; Yang, L.; Han, G.; Move, O.A. RAQ–A random forest approach for predicting air quality in urban sensing systems. *Sensors* **2016**, *16*, 86. [CrossRef] [PubMed]
17. Pérez, P.; Trier, A.; Reyes, J. Prediction of PM2. 5 concentrations several hours in advance using neural networks in Santiago, Chile. *Atmos. Environ.* **2000**, *34*, 1189–1196. [CrossRef]
18. Corani, G. Air quality prediction in Milan: Feed-forward neural networks, pruned neural networks and lazy learning. *Ecol. Model.* **2005**, *185*, 513–529. [CrossRef]
19. Hrust, L.; Klaić, Z.B.; Križan, J.; Antonić, O.; Hercog, P. Neural network forecasting of air pollutants hourly concentrations using optimised temporal averages of meteorological variables and pollutant concentrations. *Atmos. Environ.* **2009**, *43*, 5588–5596. [CrossRef]
20. Paschalidou, A.K.; Karakitsios, S.; Kleanthous, S.; Kassomenos, P.A. Forecasting hourly PM10 concentration in Cyprus through artificial neural networks and multiple regression models: Implications to local environmental management. *Environ. Sci. Pollut. Res.* **2011**, *18*, 316–327. [CrossRef]
21. Liu, H.; Li, Q.; Yu, D.; Gu, Y. Air quality index and air pollutant concentration prediction based on machine learning algorithms. *Appl. Sci.* **2019**, *9*, 4069. [CrossRef]
22. General Authority for Statistics, S.A. Population Characteristics Surveys 2017. Available online: https://www.stats.gov.sa/en/5655 (accessed on 1 November 2017).
23. Shafi, S.; Dar, O.; Khan, M.; Khan, M.; Azhar, E.I.; McCloskey, B.; Zumla, A.; Petersen, E. The annual Hajj pilgrimage—Minimizing the risk of ill health in pilgrims from Europe and opportunity for driving the best prevention and health promotion guidelines. *Int. J. Infect. Dis.* **2016**, *47*, 79–82. [CrossRef]
24. Islam, M.S.; Ekiz, E.; Buhalis, D. Hajj and Umrah. In *Encyclopedia of Tourism Management and Marketing*; Edward Elgar Publishing: Cheltenham, UK, 2022; pp. 485–489.
25. Habeebullah, T.M. An Analysis of Air Pollution in Makkah-a View Point of Source Identification. *Environ. Asia* **2013**, *2*, 11–17.
26. Abdou, A.E.A. Temperature Trend on Makkah, Saudi Arabia. *Atmos. Clim. Sci.* **2014**, *2014*, 48254. [CrossRef]
27. Lelieveld, J.; Evans, J.S.; Fnais, M.; Giannadaki, D.; Pozzer, A. The contribution of outdoor air pollution sources to premature mortality on a global scale. *Nature* **2015**, *525*, 367–371. [CrossRef] [PubMed]
28. Bruno, F.; Cocchi, D. A unified strategy for building simple air quality indices. *Environmetrics* **2002**, *13*, 243–261. [CrossRef]